

This is the accepted manuscript made available via CHORUS. The article has been published as:

# Detailed Mapping of the Local $\text{Ir}^{4+}$ Dimers through the Metal-Insulator Transitions of $\text{CuIr}_2\text{S}_4$ Thiospinel by X-Ray Atomic Pair Distribution Function Measurements

E. S. Božin, A. S. Masadeh, Y. S. Hor, J. F. Mitchell, and S. J. L. Billinge

Phys. Rev. Lett. **106**, 045501 — Published 24 January 2011

DOI: [10.1103/PhysRevLett.106.045501](https://doi.org/10.1103/PhysRevLett.106.045501)

# Study of the local $\text{Ir}^{4+}$ dimers through the metal-insulator transitions of $\text{CuIr}_2\text{S}_4$ by x-ray atomic pair distribution function measurements

E. S. Božin,<sup>1,\*</sup> A. S. Masadeh,<sup>2,3</sup> Y. S. Hor,<sup>4,†</sup> J. F. Mitchell,<sup>4</sup> and S. J. L. Billinge<sup>1,5</sup>

<sup>1</sup>*Condensed Matter Physics and Materials Science Department,*

*Brookhaven National Laboratory, Upton, NY 11973\**

<sup>2</sup>*Department of Physics and Astronomy, Michigan State University, East Lansing, MI 48824*

<sup>3</sup>*Department of Physics, University of Jordan, Amman 11942, Jordan*

<sup>4</sup>*Materials Science Division, Argonne National Laboratory, Argonne, Illinois 60439 † and*

<sup>5</sup>*Department of Applied Physics and Applied Mathematics, Columbia University, New York, NY 10027*

The evolution of the *short range* structural signature of  $\text{Ir}^{4+}$  dimer state in  $\text{CuIr}_2\text{S}_4$  thiospinel has been studied across the metal-insulator phase transitions as the metallic state is induced by temperature, Cr-doping, and x-ray fluence. An atomic pair distribution function (PDF) approach reveals that there are no *local* dimers that survive into the metallic phase when this is invoked by temperature and doping. The PDF shows  $\text{Ir}^{4+}$  dimers when they exist, regardless of whether or not they are long-range ordered. At 100 K, exposure to 98 keV x-ray beam melts the long range dimer order within a few seconds, though the local dimers remain intact. This shows that the metallic state accessed on warming and doping is qualitatively different from the state obtained under x-ray irradiation.

PACS numbers: 75.50.2y, 61.80.Cb,

Local fluctuations in electronic and magnetic states are important in systems exhibiting colossal responses such as high temperature superconductors (HTS) [1, 2] and colossal magnetoresistive (CMR) materials [3–5]. However, the ubiquity of these fluctuations and the exact role that they play in the rich observed physical phenomena are not understood. Part of the reason is that such fluctuations are extremely difficult to study because they are not long-range ordered [6, 7]. In cases where there is strong electron-phonon coupling a signature of the local electronic states is evident in the local atomic structure and the electronic or magnetic states may be studied using a local structural probe [8, 9] such as the atomic pair distribution function (PDF) analysis of powder diffraction data [10, 11]. Here we use the PDF to study directly the existence or absence of  $\text{Ir}^{4+}$  dimer-states in  $\text{CuIr}_2\text{S}_4$ , which yields essential information to understand the unusual and poorly understood metal insulator transitions in this system.

$\text{CuIr}_2\text{S}_4$  has generated significant interest recently because of its unusual magnetic, electronic and structural behavior [12–17]. It exhibits a metal-insulator (MI) transition, accompanied by a dramatic loss in magnetic susceptibility, charge ordering, and an accompanying structural phase transition, making it an important system for studying the interplay of electronic, magnetic, orbital and structural degrees of freedom. On cooling, crystallography indicates that the structural change in the insulating phase accompanies the formation of  $\text{Ir}^{4+}$  dimers (pairs of iridium ions move closer together by 0.5 Å [16]), which are presumably magnetic singlets explaining the loss of magnetic susceptibility. As well as the metallic phase appearing on warming, the material also becomes more metallic when doped with Cr [18] and irradiated with

optical [19] and x-ray [20, 21] illumination.

The metallic state above the insulating ordered-dimer state in the phase diagram is unusual. It has a non-conventional conduction mechanism [22] and a recent observation of weak Fermi edges and broad peak features in ultraviolet photoemission spectra suggest that fluctuating dimers may survive in the high temperature metallic phase [23]. A PDF study can address this directly since the PDF is sensitive to the existence of the dimers whether or not they are ordered [23]. The local dimers are clearly evident in the PDF because of the large (0.5 Å) change in the Ir-Ir bond-length in the dimer which separates this peak from any other nearby peak in the PDF. Here we show definitively that the dimers disappear abruptly from the local structure at the metal-insulator transition on warming [16]. They also disappear as the MI transition is crossed on doping Cr. However, they survive locally through an x-irradiation induced insulator-metal transition at low temperature [20, 24]. These results provide essential input to guide theories of these interesting metal-insulator transitions [25, 26].

$\text{CuIr}_2\text{S}_4$  and  $\text{Cu}(\text{Ir}_{0.95}\text{Cr}_{0.05})_2\text{S}_4$  were prepared by solid state reaction in sealed, evacuated quartz ampoules. Stoichiometric quantities of the metals and elemental sulfur were thoroughly mixed, pelletized, and sealed under vacuum. The ampoules were slowly heated to 650-750 °C and held at this temperature for several weeks with intermediate grinding and pressing. The products were found to be single phase based on x-ray powder diffraction.

Total scattering experiments to obtain  $\text{CuIr}_2\text{S}_4$  PDFs were performed at the 6-ID-D beam-line at the Advanced Photon Source at Argonne National Laboratory, with 98.136 keV x-rays using the rapid acquisition (RAPDF) mode [27]. The setup utilized a General Electric amor-

phous silicon-based area detector and Oxford Cryosystems cryostream for temperature variation with a sample to detector distance of 268.620 mm. Samples were packed in a kapton capillary 1 mm in diameter. The data were collected at various temperatures between 100 K and 300 K. The exposure time was varied as specified further in the text. The raw 2D data were integrated and converted to intensity versus  $2\theta$  using the software Fit2D [28], where  $2\theta$  is the diffraction angle. The integrated data were corrected for experimental artifacts, normalized, and Sine Fourier transformed (FT) to the PDF,  $G(r)$ , based on standard methods [11] using the program PDFgetX2 [29]. The upper limit of momentum transfer used in the FT of  $Q_{max} = 23.0 \text{ \AA}^{-1}$  was optimized such as to avoid large termination effects on the one hand and statistical noise on the other.

PDFs from  $\text{CuIr}_2\text{S}_4$  are shown in Fig. 1. The peak in the PDF coming from the  $\text{Ir}^{4+}\text{-Ir}^{4+}$  dimers (indicated by the arrow) is clearly apparent in the right-hand panels where the PDFs are shown on an expanded scale. The size of the distortion coupled with the fortuitous absence of other atomic distances at the same place allows us to study the dimer state in a model independent way using the PDF. Additionally, the changes in the next near-neighbor peak centered at  $3.5 \text{ \AA}$  clearly indicate that there is also an accompanying redistribution of PDF intensity from this peak to the dimer peak, lending confidence that the PDF is sensitive to the presence of local dimers. This is especially clear in the difference curve shown offset below. The  $3.0 \text{ \AA}$  PDF peak is not evident in the metallic state on warming (red curve in Fig. 1(a)) indicating that there are no local dimers in the metallic phase accessed by increasing temperature.

We now investigate the local structural changes on traversing the MI transitions. Fig. 1(a) shows the effect of the temperature induced MI transition: experimental PDFs of  $\text{CuIr}_2\text{S}_4$  in the metallic state at 230 K (red) and in the insulating state at 220 K (blue), 10 K apart, are dramatically different in the entire range, as evident from their difference curve (green) indicating that the structural change occurs at all length-scales. Normal thermal effects have a much smaller effect on the PDF as is evident from Fig. 1(b), where the differences in the PDF due to a 10 K temperature change in the same structural phase (metallic state in this case), are within the estimated uncertainties of the measurement. There is clearly a significant structural modification in the local structure, as well as the average structure [16], at the MI transition. This may not seem surprising but this is not always the case, for example in systems where distortions persist but become disordered at high temperature [30].

In Fig. 2 we show the detailed temperature dependence of the  $3.0 \text{ \AA}$  dimer peak as the sample goes through the MI transition. The main panel shows the change in the peak maximum, defined as  $\Delta G(T) = G(T) - G(230)$ , versus temperature for both cooling (solid blue symbols)

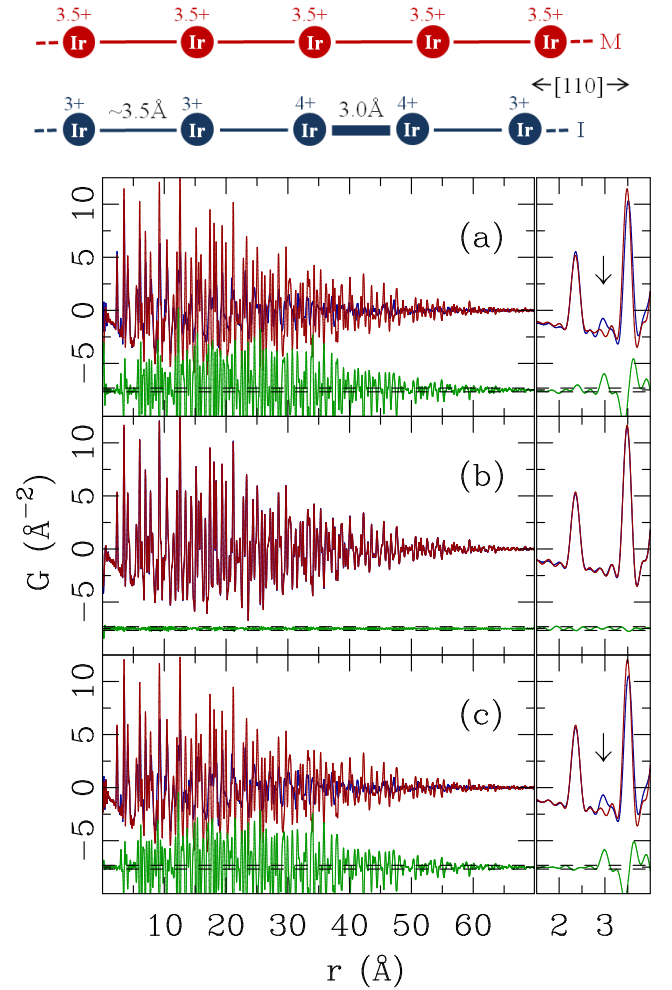


FIG. 1. (Color online) Changes in PDF across the MI transition in  $\text{CuIr}_2\text{S}_4$  when induced by temperature and Cr-doping: experimental PDFs of (a) metallic 230 K (red) and insulating 220 K (blue), (b) metallic 230 K (red) and metallic 240 K (blue), (c) insulating undoped (blue) and metallic 5% Cr-doped (red) at 200 K temperature. Difference curves are shown offset below (green). The corresponding side panels emphasize the short-range scale: the appearance of excess PDF intensity corresponding to the short  $\text{Ir}^{4+}\text{-Ir}^{4+}$  dimer distance around  $3.0 \text{ \AA}$  in the insulating phase is indicated by arrows. The existence of this peak indicates the presence of local dimers. For reference, a sketch of Ir-chains in M and I phases is given on top. See text for details.

and warming (solid red symbols) cycles. To demonstrate the reproducibility of the data, the evolution of the dimer peak in the PDF itself is shown for cooling and warming cycles in lower left and upper right insets, respectively. Clean hysteretic behavior is observed, with a square loop that is about 10 K wide, in accord with hysteretic behavior observed in magnetic [31, 32] and transport measurements [14, 18, 20, 33, 34]. Not only is long range dimer order destroyed at the MI transition, but local dimers also disappear.

The metallic state can also be reached from insulat-

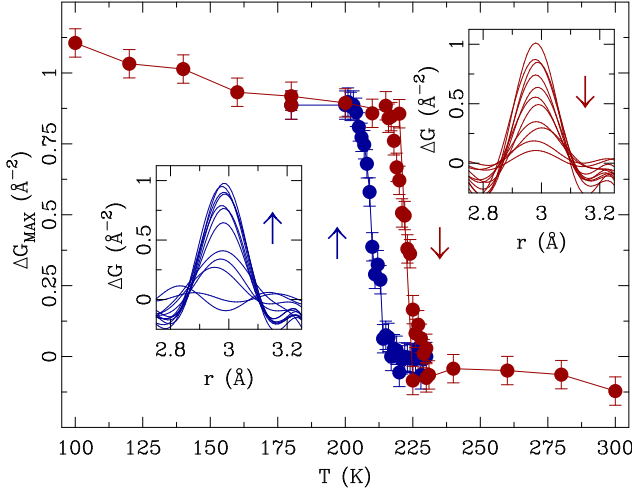


FIG. 2. (Color online) Evolution of the short-range dimer structure across the MI transition in  $\text{CuIr}_2\text{S}_4$  induced on cooling (blue) and warming (red) cycles. The insets show the evolution of the 3.0 Å dimer PDF peak on cooling (bottom left) and warming (up right). The main panel shows the excess height of this peak with respect to the 230 K data (see text for details).

ing  $\text{CuIr}_2\text{S}_4$  by substituting a small percentage of Ir with Cr [18]. Inspection of Figure 1(c), which shows the differences in two PDFs corresponding to insulating  $\text{CuIr}_2\text{S}_4$  (blue solid line) and metallic  $\text{Cu}(\text{Ir}_{0.95}\text{Cr}_{0.05})_2\text{S}_4$  (red solid line) at 200 K, indicates that the local dimers also disappear in the local structure in the metallic state accessed by 5% Cr-substitution at fixed temperature.

Here we extend the study to the destruction of the insulating ordered dimer state by x-ray irradiation [19–21]. Photo-induced phase transitions, with an associated change in properties, are an important area of research because of the possibility of controlling properties optically [35, 36]. The structural response to x-ray irradiation of our  $\text{CuIr}_2\text{S}_4$  sample is summarized in Fig. 3 as the exposure time is varied at  $T = 100$  K. Panels (a), (b), (c), and (d) each show a quarter of a full 2D diffraction pattern for exposures of 0.5 s, 1.0 s, 30.0 s, and 0.5 s, where the exposures were taken one after each other in the order (a)-(d) but with a 2 minute gap between each where the sample was not being irradiated (shutter closed). The 1-D diffraction patterns shown in panels (e) and (f) are obtained by integrating around the circular Debye-Scherrer rings on the 2-D detector, evident in Fig. 3(a)-(d). An extra peak can be seen in the diffraction pattern, indicated by the arrow in panel (b) and evident in the integrated data, inset in panel (f). This comes from long-range ordered dimers in the structure, but due to the limited reciprocal space resolution of the RAPDF measurement [27] it is formed from several super-lattice peaks (SLP), including the strong  $(3/2, 3/2, 3/2)$  peak. This is observed in all but image (c) that corresponds to the longest exposure time, reflecting the fact that the

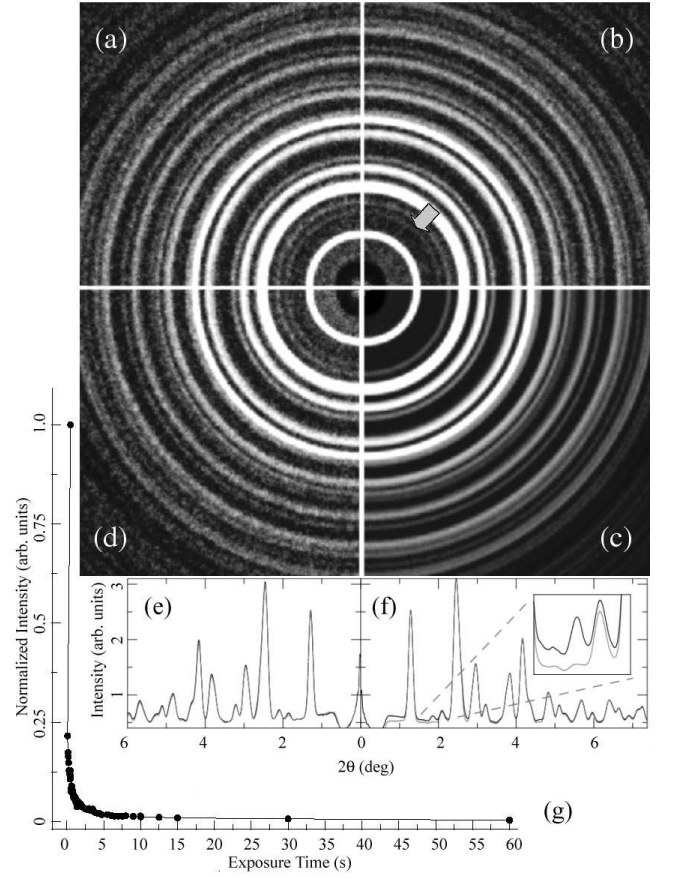


FIG. 3. Raw 2D diffraction data at 100 K of  $\text{CuIr}_2\text{S}_4$  for successive (a) 0.5 s, (b) 1.0 s, (c) 30.0 s, and (d) 0.5 s exposures to x-rays, with 2 minute separations between the exposures. Notable is an extra diffraction ring indicated by the arrow in panel (b) present for all exposure times shown, except for 30 s. This corresponds to an unresolved multiplet of SLPs, including  $(3/2, 3/2, 3/2)$ , coming from long range charge and dimer order. Panels (e) and (f) show the 1D powder diffraction pattern obtained by integrating around the rings from panels (a), (d) and (b), (c) respectively. The inset in panel (f) emphasizes the disappearance of the SLP multiplet. (g) Dependence of the normalized SLP intensity vs x-ray exposure time.

long range dimer order is melted in this case. Notable also is an immediate recovery of the long range order at 100 K in the successive 0.5 s exposure upon cessation of the exposure. Finally, in Fig. 3(g) we show the normalized integrated intensity of this multiplet SLP as a function of the x-ray exposure time. This establishes the behavior of the long-range dimer of our sample and has a behavior similar to other studies [20], but at a decay rate that is about two orders of magnitude faster than the one observed earlier. This may be a result of the different temperature of measurement (100 K vs 10 K) or the different energy or flux of the irradiating x-rays (100 keV vs. 8 keV) [20].

The conductivity of the irradiated state increases over



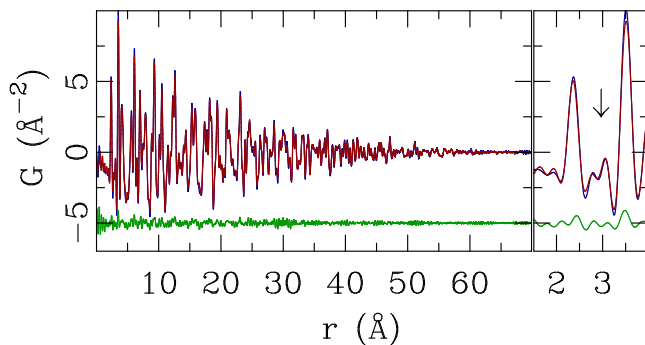


FIG. 4. (Color online) Experimental PDFs of  $\text{CuIr}_2\text{S}_4$  at 100 K corresponding to short (250 msec, blue) and long (30 sec, red) exposure times. The difference curve is offset below for clarity. The side panel emphasizes the short-range structure, with the arrow denoting the position of the 3.0 Å PDF peak corresponding to the local dimers. The differences are much smaller than seen in Fig. 1.

that of the insulating ground-state, though to a lesser degree than at the temperature or Cr induced MI transition [18]. We would like to see if the PDF yields information about the existence of local dimers in this more metallic state induced by irradiation and so we compared the local structures after short and long x-ray exposures.

Fig. 4 shows a comparison of the PDFs obtained in the first 250 ms of x-ray exposure, and after 30 seconds of irradiation. As discussed above, the superstructure observed in the x-ray diffraction pattern coming from the dimer order is observed in the data from 250 ms but is completely destroyed in the data obtained after 30s of irradiation. However, although the average structure behaves the same way at this MI transition, the behavior of the local structure is completely different between the irradiation induced and temperature or doping induced transitions. A comparison of Fig. 1 and Fig. 4 dramatically illustrates that the local structure is preserved on irradiation, where it is significantly changed at the temperature/doping transition. There is no loss in intensity of the dimer peak in the PDF after long irradiation suggesting that all charges remain localized resulting in distinct  $\text{Ir}^{3+}$  and  $\text{Ir}^{4+}$  sites, but further, that the localized holes remain bound in dimers. The increased conductivity in the irradiated sample [20, 21] must be due to an increased hopping rate of localized charges bound in the dimer pairs that are no longer pinned to the lattice in an ordered arrangement and the irradiation must facilitate this pair-hopping.

These PDF measurements allow us to measure directly if the  $\text{Ir}^{4+}$ - $\text{Ir}^{4+}$  dimers exist regardless of whether or not they are long range ordered. We show unambiguously that local dimers disappear in the metallic phases accessed on warming and on Cr doping, but they persist in the metallic state induced by irradiation with x-rays.

We would like to thank P. Chupas and K. Chapman

for their help in data collection. Work in the Billinge-group was supported by the Office of Science, U.S. Department of Energy, under contract no. DE-AC02-98CH10886. Data were collected at the 6ID-D beamline at the Advanced Photon Source at the Argonne National Laboratory supported under DOE contract No. DE-AC02-06CH11357. EB and AM dedicate this article to their prematurely departed colleague and friend Mustafa Al-Hajdarwish.

\* bozin@bnl.gov

† current address: Department of Physics, Missouri University of Science and Technology, Rolla, MO 65409, USA

- [1] S. H. Pan et al., *Nature* **413**, 282 (2001).
- [2] S. Takeshita et al., *Phys. Rev. Lett.* **103**, 027002 (2009).
- [3] E. Dagotto, *Science* **309**, 257 (2005).
- [4] J. Tao et al., *Phys. Rev. Lett.* **103**, 097202 (2009).
- [5] S. J. L. Billinge et al., *Phys. Rev. Lett.* **77**, 715 (1996).
- [6] S. J. L. Billinge and I. Levin, *Science* **316**, 561 (2007).
- [7] M. Hennion et al., *Phys. Rev. Lett.* **94**, 057006 (2005).
- [8] J. Lee et al., *Nature* **442**, 546 (2006).
- [9] E. S. Bozin et al., *Phys. Rev. Lett.* **98**, 137203 (2007).
- [10] S. J. L. Billinge, *J. Solid State Chem.* **181**, 1698 (2008).
- [11] T. Egami and S. J. L. Billinge, *Underneath the Bragg peaks: structural analysis of complex materials*, Pergamon Press, Elsevier, Oxford, England, 2003.
- [12] T. Furubayashi et al., *J. Phys. Soc. Jpn* **63**, 3333 (1994).
- [13] J. Matsuno et al., *Phys. Rev. B* **55**, R15979 (1997).
- [14] S. Nagata et al., *Phys. Rev. B* **58**, 6844 (1998).
- [15] H. Ishibashi et al., *J. Magn. Magn. Mater.* **226-230**, 233 (2001).
- [16] P. G. Radaelli et al., *Nature* **416**, 155 (2002).
- [17] M. Croft et al., *Phys. Rev. B* **67**, 201102 (2003).
- [18] R. Endoh et al., *Phys. Rev. B* **68**, 115106 (2003).
- [19] K. Takubo et al., *Phys. Rev. Lett.* **95**, 246401 (2005).
- [20] H. Ishibashi et al., *Phys. Rev. B* **66**, 144424 (2002).
- [21] T. Furubayashi et al., *Solid State Commun.* **126**, 617 (2003).
- [22] A. T. Burkov et al., *Phys. Rev. B* **61**, 10049 (2000).
- [23] K. Takubo et al., *Phys. Rev. B* **78**, 245117 (2008).
- [24] V. Kiryukhin et al., *Phys. Rev. Lett.* **97**, 225503 (2006).
- [25] K. Kitamoto et al., *Phys. Rev. B* **68**, 195124 (2003).
- [26] D. I. Khomskii and T. Mizokawa, *Phys. Rev. Lett.* **94**, 156402 (2005).
- [27] P. J. Chupas et al., *J. Appl. Crystallogr.* **36**, 1342 (2003).
- [28] A. P. Hammersley et al., *High Pressure Res.* **14**, 235 (1996).
- [29] X. Qiu et al., *J. Appl. Crystallogr.* **37**, 678 (2004).
- [30] H. J. Kim et al., *Phys. Rev. Lett.* **96**, 226401 (2006).
- [31] P. Somasundaram et al., *J. Appl. Phys.* **83**, 7243 (1998).
- [32] H. Suzuki et al., *J. Phys. Soc. Jpn* **68**, 2495 (1999).
- [33] S. Nagata et al., *Physica B* **194-196**, 1077 (1994).
- [34] V. N. Andreev et al., *Phys. Status Solidi B* **234**, 623 (2002).
- [35] S. Koshihara and S. Adachi, *J. Phys. Soc. Jpn* **75**, 011005 (2006).
- [36] S. Iwai et al., *Phys. Rev. Lett.* **96**, 057403 (2006).